

Hypermodularity and community detection in higher-order networks

Charo I. del Genio^{1,2}

¹*Institute of Smart Agriculture for Safe and Functional Foods and Supplements, Trakia University, Stara Zagora 6000, Bulgaria*

²*Research Institute of Interdisciplinary Intelligent Science,
Ningbo University of Technology, 315104, Ningbo, China*

(Dated: December 11, 2024)

Numerous networked systems feature a structure of non-trivial communities, which often correspond to their functional modules. Such communities have been detected in real-world biological, social and technological systems, as well as in synthetic models thereof. While much effort has been devoted to develop methods for community detection in traditional networks, the study of community structure in networks with higher-order interactions is still relatively unexplored. In this article, we introduce a formalism for the hypermodularity of higher-order networks that allows us to use spectral methods to detect community structures in hypergraphs. We apply this approach to synthetic random networks as well as to real-world data, showing that it produces results that reflect the nature and the dynamics of the interactions modelled, thereby constituting a valuable tool for the extraction of hidden information from complex higher-order data sets.

I. INTRODUCTION

Many complex systems have the structure of a network, in which pairs of elements of a discrete set, called the nodes, are connected when they share a common property [1–4]. Typically, such networks have structural features with different characteristic length scales. The smallest length scale is that of the number of links (also called edges) of a given node, which takes the name of degree. The link between the neighbours of a specific node define the local neighbourhood structure, which is the next larger length scale. As one considers the whole network, one may find sets of nodes whose elements have more connections amongst themselves than they have with nodes in other such sets. When this happens, these mesoscale sets take the name of communities, and the network is said to exhibit a non-trivial community structure. The presence of network communities has been detected in a large number of real-world systems, such as protein networks, social networks and food webs, as well as in synthetic models of complex systems of diverse nature [5–14]. In general, the community structure of a network affects the behaviour of the system, and often one can trace a direct correspondence between communities and structural units responsible for specific functions.

As a result, a large number of methods have been developed to detect communities in networks [14, 15]. A particularly successful approach is the maximization of a quality function that measures how pronounced a partition of a network into communities is by computing the difference between the density of the observed intra-community links and that of a suitably chosen null model. The most commonly used such function is called *modularity* [16]. However, finding the network partition that maximizes it is an NP-hard computational problem [17]. Thus, large efforts have been devoted to creating algorithms that provide the best possible approximation to the global maximum in a workable running time [18–27].

Recently, however, it has become increasingly clear that dyadic interactions are only a part of the important

relationships that occur in complex systems. In fact, researchers have recognized the relevance of collective interactions for the functioning of systems as diverse as social groups, neural networks and multi-species assemblages of microorganisms, sparking a new interest in structures with higher-order interactions [28, 29]. As a result, the main type of structural backbone that is currently generating considerable attention is no longer that of a graph, but rather that of a hypergraph. In hypergraphs, edges do not necessarily connect pairs of elements, but rather they can connect triplets, quadruplets, or any other number of nodes [30].

Unfortunately, the landscape of research on the subject of community detection in hypergraphs is not well developed, with only a few methods available, mostly dynamical in nature, or based on stochastic block models, or using projections [31–34]. These choices are probably due to the inherent difficulty of operating on a structure that requires tensor methods without projecting it. An exception to these approaches is an extension to hypergraphs of the Chung-Lu model, which results in a modularity measure that is closely related to the one originally used in traditional networks [35]. However, perhaps due to the specific choice of formalism used, this last work limits itself to an adaptation of the Louvain algorithm [20].

Here, we introduce and characterize modularity for hypergraphs using a formalism that allows us to create a spectral algorithm for its maximization. The possibility of developing such a method rests on a derivation we offer of a closed-form combinatorial expression that enables us to write the hypermodularity equation in vector form. We then validate our method by analyzing random hypergraphs and real-world higher-order networks, showing that it detects communities that correspond to similarity of cognitive processes in people and reflect the underlying social dynamics.

II. RESULTS

A. Hypermodularity

In a fully general case, a hypergraph may contain edges involving different numbers of nodes. If all the edges have the same size k , the hypergraph is called k -uniform. Note that this means that classic networks with only dyadic interactions are 2-uniform hypergraphs. However, each edge size is independent from all the others, and they all correspond to different specific orders of many-body interactions. Thus, a hypergraph H can be thought of as the union of multiple independent uniform sub-hypergraphs, each consisting of edges of a single size. In turn, this consideration also applies to the task of finding the community structure of H , since, for example, a group of nodes may form strong 3-body interactions but no significant pairwise ones. Therefore, in the following we study the problem on uniform hypergraphs, since a solution on them also provides one to the general case.

The idea behind classic network modularity is to exploit a measure based on the difference between the number of observed edges between two nodes and the one that would be expected if the placement of all the edges in the graph were randomized while keeping the degrees of the nodes unchanged. Given a partition of a network with N nodes and m edges into a set of communities, this approach results in the following expression for the modularity Q [16]:

$$Q = \frac{1}{2m} \sum_{i=1}^N \sum_{j=1}^N \left[\left(A_{i,j} - \frac{d_i d_j}{2m} \right) \delta_{C_i, C_j} \right], \quad (1)$$

where \mathbf{A} is the adjacency matrix, d_i is the degree of node i , δ is Kronecker's symbol and C_i is the community to which node i has been assigned. Applying the same idea to a k -uniform hypergraph, we introduce an expression for the *hypermodularity* of a partition:

$$Q = \frac{1}{k!m} \sum_{\{v_1, \dots, v_k\}} \left[\left(A_{v_1, \dots, v_k} - \frac{(k-1)!}{(km)^{k-1}} \prod_{i=1}^k d_{v_i} \right) \prod_{\substack{i,j=1 \\ i \neq j}}^k \delta_{C_{v_i}, C_{v_j}} \right]. \quad (2)$$

In the formula above, \mathbf{A} is the adjacency tensor of the hypergraph, the combinatorial factor before the product of degrees accounts for the number of available ways to join nodes of given degrees in an edge, and the sum is on all the possible choices of k nodes, allowing for repetitions. Thus, the expression directly measures the difference between the number of hyperedges of size k that are found amongst the nodes in each community and the number that would be expected if the same hyperedges had been

placed at random. The task is thus to find the partition of the network that maximizes Q . Note that \mathbf{A} is more precisely described as a hypermatrix, rather than a tensor, since it does not represent a multilinear application. However, with a slight abuse of notation we will still refer to it as a tensor, as this is the most commonly adopted terminology, especially in the applied literature. Also note that, for $k = 2$, the expression reduces to that of graph modularity, which becomes therefore a special case of this more general formulation, as desired.

The principal difference between the hypermodularity of Eq. (2) and the classic modularity for graphs is in the fact that the latter can be cast into a pure matrix equation, whereas such an expression cannot be obtained straightforwardly in the hypergraph case. Thus, one cannot directly use the same methods employed on traditional networks to produce a bipartition, which is a starting step in many community detection algorithms.

B. Spectral partitioning

To solve this problem, first note that if the hypergraph is simple, meaning that it does not have multiple edges, as it is often the case in real-world structures, then one can write $A_{v_1, \dots, v_k} = \mathbf{1}_{(v_1, \dots, v_k) \in H}$, where $\mathbf{1}$ is an indicator variable whose value is 1 if the edge (v_1, \dots, v_k) belongs to H and 0 otherwise. Thus, Eq. (2) can be rewritten as

$$Q = \frac{1}{k!m} \sum_{\{v_1, \dots, v_k\}} \left[\left(\mathbf{1}_{(v_1, \dots, v_k) \in H} - \frac{(k-1)!}{(km)^{k-1}} \prod_{i=1}^k d_{v_i} \right) \prod_{\substack{i,j=1 \\ i \neq j}}^k \delta_{C_{v_i}, C_{v_j}} \right]. \quad (3)$$

But then, one can consider the whole term within the round brackets in the equation above as a hypersymmetric data tensor \mathbf{B} , which, in principle, can be analyzed using higher-order singular-value decomposition (SVD), whose applications to data science and machine learning have proved to be very fruitful [36–40]. Given a data tensor, its higher-order SVD is a compact SVD carried out on one of its standard flattenings. These are dimensional reductions of the tensor that compact all its dimensions, except for an arbitrarily chosen one, into a single dimension. In our case, this means that the standard flattenings of \mathbf{B} are the matrices $\mathbf{E}^{(i)}$ defined by

$$E_{v_i, (v_1, v_2, \dots, v_{i-1}, v_{i+1}, \dots, v_k)}^{(i)} = \mathbf{1}_{(v_1, \dots, v_k) \in H} - \frac{(k-1)!}{(km)^{k-1}} \prod_{j=1}^k d_{v_j}, \quad (4)$$

where i is any integer from 1 to k . Note that, effectively, the column index of $\mathbf{E}^{(i)}$ is a sort of collective index,

which can take a number of values that is equal to the number of all possible combinations of allowed values for all the indices of \mathbf{B} except the i -th one. Also note that, with these manipulations, we do not neglect or discard any information that is present in the initial equation.

In general, the compact SVD of an $N \times M$ matrix \mathbf{X} provides three matrices \mathbf{U} , $\mathbf{\Sigma}$ and \mathbf{V} such that $\mathbf{X} = \mathbf{U}\mathbf{\Sigma}\mathbf{V}^\dagger$, where \dagger indicates Hermitian conjugation. More specifically, \mathbf{U} and $\mathbf{\Sigma}$ are $N \times N$ and \mathbf{V} is $M \times N$. Also, the columns of \mathbf{U} and those of \mathbf{V} are the left singular vectors and the right singular vectors of \mathbf{X} , respectively, whereas $\mathbf{\Sigma}$ is diagonal and it contains the (positive) singular values of \mathbf{X} . For our purposes, the procedure is useful because, since \mathbf{B} is real, so are its flattenings $\mathbf{E}^{(i)}$. This means that the Hermitian conjugation reduces to transposition, and that the matrix \mathbf{U} is guaranteed to be real and orthogonal. Thus, if we could establish a relation between the product of Kronecker deltas in Eq. (3) and some vector quantities encoding the assignments of the nodes into communities, we would be able to maximize the hypermodularity by imposing the partition described by the left singular vector corresponding to the largest singular value.

To find this vector, one can use a variety of methods. However, since we are only interested in the first left singular vector, we can use an equivalent of the power iteration, thus avoiding the need of performing a full decomposition. The procedure is as follows. First, create an initial N -dimensional vector \mathbf{z}_0 whose components are standard normal random variables. Normalize \mathbf{z}_0 , and compute the vector $\mathbf{z}_1 = \mathbf{E}^{(i)} \left(\mathbf{E}^{(i)\top} \mathbf{z}_0 \right)$, where \top indicates transposition. Normalize \mathbf{z}_1 and repeat the multiplication to obtain \mathbf{z}_2 . After a large number of iterations, the resulting vector \mathbf{z}_∞ is the first left singular vector of $\mathbf{E}^{(i)}$. Then, one can determine the community assign-

ment based on the signs of the elements of the vector: if the i th element is positive, assign node i to the first community; if it is negative, assign it to the second one.

However, before applying this method, we need to answer two questions. The first one is how to determine which one of the k possible flattenings to use for the SVD.

C. Identity of the flattenings

To answer the question, start by explicitly writing the k -th standard flattening of \mathbf{B} :

$$\mathbf{E}^{(k)} = \begin{pmatrix} B_{1,1,\dots,1} & B_{2,1,\dots,1} & \dots & B_{N,N,\dots,1} \\ B_{1,1,\dots,2} & B_{2,1,\dots,2} & \dots & B_{N,N,\dots,2} \\ \vdots & \vdots & \ddots & \vdots \\ B_{1,1,\dots,N} & B_{2,1,\dots,N} & \dots & B_{N,N,\dots,N} \end{pmatrix}. \quad (5)$$

This equation shows that the row index of $\mathbf{E}^{(k)}$ corresponds to the k -th index of \mathbf{B} . Also, the column index of $\mathbf{E}^{(k)}$, which numerically ranges from 1 to N^{k-1} , is equal to the positional number of the corresponding choice of values for the remaining indices of \mathbf{B} in an inverse lexicographic order. In other words, each element $E_{i,j}^{(k)}$ corresponds to the element of \mathbf{B} whose k -th index is equal to i and whose other indices v_1, \dots, v_{k-1} satisfy the equation

$$j = v_1 N^0 + (v_2 - 1) N^1 + (v_3 - 1) N^2 + \dots + (v_{k-1} - 1) N^{k-2}. \quad (6)$$

Effectively, the equation above provides the unique $k-1$ digits of the column numbers of the elements of $\mathbf{E}^{(k)}$ expressed in a base- N positional system.

Now consider the generic x -th standard flattening of \mathbf{B} :

$$\mathbf{E}^{(x)} = \begin{pmatrix} B_{1,1,\dots,1,1,1,\dots,1} & B_{2,1,\dots,1,1,1,\dots,1} & \dots & B_{N,N,\dots,N,1,N,\dots,N} \\ B_{1,1,\dots,1,2,1,\dots,1} & B_{2,1,\dots,1,2,1,\dots,1} & \dots & B_{N,N,\dots,N,2,N,\dots,N} \\ \vdots & \vdots & \ddots & \vdots \\ B_{1,1,\dots,1,N,1,\dots,1} & B_{2,1,\dots,1,N,1,\dots,1} & \dots & B_{N,N,\dots,N,N,N,\dots,N} \end{pmatrix}. \quad (7)$$

Here, the row index of $\mathbf{E}^{(x)}$, which is the index of \mathbf{B} that changes between the elements in each column, is the x -th one. So, given an element $E_{i,j}^{(x)}$, it corresponds to the element of \mathbf{B} whose x -th index is equal to i and whose other indices are such that

$$j = v_1 N^0 + (v_2 - 1) N^1 + \dots + (v_{x-1} - 1) N^{x-2} + (v_{x+1} - 1) N^{x-1} + \dots + (v_k - 1) N^{k-2}. \quad (8)$$

Then, fix a row index l and a column index m for the two flattenings, and take their elements $E_{l,m}^{(k)}$

and $E_{l,m}^{(x)}$. The former maps to the element of the data tensor $B_{v_1, v_2, \dots, v_{x-1}, v_x, v_{x+1}, \dots, v_{k-1}, l}$ whose last index is equal to l and whose other indices correspond to the unique decomposition of m in powers of N . The other, in the same way, corresponds instead to $B_{v_1, v_2, \dots, v_{x-1}, l, v_{x+1}, \dots, v_k}$. Thus, the indices of the latter element of \mathbf{B} are a permutation of those of the former. But, since \mathbf{B} is hypersymmetric, $B_{v_1, v_2, \dots, v_{x-1}, v_x, v_{x+1}, \dots, v_{k-1}, l} = B_{v_1, v_2, \dots, v_{x-1}, l, v_{x+1}, \dots, v_k}$, which, in turn, means that, for any choice of l and m , $E_{l,m}^{(x)} = E_{l,m}^{(k)}$ for all x . Thus, all the standard flattenings

of the data tensor of a simple hypergraph are identical, and in the following we use the k -th ones without loss of generality, omitting explicit mention of the dimension used for their construction.

D. Building a vector equation

The next task on the road to building a method for spectral bisection of a higher-order network is finding a way to express Eq. (3) in terms of vector quantities. To start, recall that one can write the simple Kronecker delta of Eq. (1) as

$$\delta_{C_i, C_j} = \frac{1}{2} (s_i s_j + 1), \quad (9)$$

where s_i are spin-like community-identifying variables that can take the values $+1$ and -1 , depending on the community to which node i is assigned. Next, note that, given k nodes, the product of deltas in Eq. (3) does not need to include all $\binom{k}{2}$ possible combinations thereof. In fact, because of transitivity of equality, the product is best expressed as a chain, so that

$$\prod_{\substack{i,j=1 \\ i \neq j}}^k \delta_{C_{v_i}, C_{v_j}} = \delta_{C_{v_1}, C_{v_2}} \delta_{C_{v_2}, C_{v_3}} \cdots \delta_{C_{v_{k-1}}, C_{v_k}}. \quad (10)$$

Then, use Eq. (9) to explicitly rewrite the product chain for $k = 3$:

$$\begin{aligned} \delta_{C_{v_1}, C_{v_2}} \delta_{C_{v_2}, C_{v_3}} &= \frac{1}{2} (s_1 s_2 + 1) \frac{1}{2} (s_2 s_3 + 1) \\ &= \frac{1}{4} (s_1 s_2^2 s_3 + s_1 s_2 + s_2 s_3 + 1). \end{aligned} \quad (11)$$

Note that in the equation above, s_1 , s_2 and s_3 indicate the community assignments of the nodes chosen as v_1 , v_2 and v_3 , and *not* those of nodes 1, 2 and 3. Thus, for $k = 3$, Eq. (3) becomes

$$\begin{aligned} Q &= \frac{1}{3!m} \sum_{\{v_1, v_2, v_3\}} \left(B_{v_1, v_2, v_3} \prod_{\substack{i,j=1 \\ i \neq j}}^3 \delta_{C_{v_i}, C_{v_j}} \right) \\ &= \frac{1}{3!m} \sum_{\{v_1, v_2, v_3\}} \left[B_{v_1, v_2, v_3} \frac{1}{4} (s_1 s_2^2 s_3 + s_1 s_2 \right. \\ &\quad \left. + s_2 s_3 + 1) \right] \\ &= \frac{1}{3!m} \sum_{\{v_1, v_2, v_3\}} \left[B_{v_1, v_2, v_3} \frac{1}{4} (s_1 s_3 + s_1 s_2 \right. \\ &\quad \left. + s_2 s_3 + 1) \right], \end{aligned} \quad (12)$$

where, in the last line, we have used $s_i^2 = 1$. But the sum above runs over all combinations of 3 nodes, which means that all the elements of \mathbf{B} are considered. In turn,

this means that, since the sum of all the elements of \mathbf{B} vanishes by construction, we can drop any constant term from the equation, obtaining

$$\begin{aligned} Q &= \frac{1}{3!m} \sum_{\{v_1, v_2, v_3\}} \left[B_{v_1, v_2, v_3} \frac{1}{4} (s_1 s_3 + s_1 s_2 + s_2 s_3) \right] \\ &= \frac{1}{3!m} \sum_{\{v_1, v_2, v_3\}} \left\{ B_{v_1, v_2, v_3} \frac{1}{4} [s_3 (s_1 + s_2) + s_1 s_2] \right\}. \end{aligned} \quad (13)$$

But, again because of the sum and of the nature of \mathbf{B} , the index of s_1 in the last term above is a dummy index. Thus, we can change that s_1 to s_3 , and get

$$Q = \frac{1}{3!m} \sum_{\{v_1, v_2, v_3\}} \left[B_{v_1, v_2, v_3} \frac{1}{4} s_3 (s_1 + 2s_2) \right], \quad (14)$$

which we rewrite as

$$Q = \frac{1}{3!m} \sum_{\{v_1, v_2, v_3\}} B_{v_1, v_2, v_3} S^{(3)}, \quad (15)$$

where we have put

$$S^{(3)} = \frac{1}{4} s_3 (s_1 + 2s_2). \quad (16)$$

This equation conveniently separates the three spin-like variables into a product of one of them and an expression featuring the other two. Thus, the equation for hypermodularity can be rewritten as

$$Q = \frac{1}{4 \cdot 3!m} \mathbf{s}^T \mathbf{E} \boldsymbol{\sigma}^{(3)}, \quad (17)$$

where \mathbf{s} is a vector containing the community assignments of all nodes, and $\boldsymbol{\sigma}^{(3)}$ is an N^2 -dimensional vector whose elements are the values of the expression $s_1 + 2s_2$ computed for all possible pairs of nodes in the same order as those corresponding to the columns of \mathbf{E} .

To find a general-use formula, repeat the calculation for $k = 4$, by writing the chain product of deltas in terms of spin-like variables, dropping any constants and replacing dummy indices with the 4th one:

$$\begin{aligned} S^{(4)} &= \delta_{C_{v_1}, C_{v_2}} \delta_{C_{v_2}, C_{v_3}} \delta_{C_{v_3}, C_{v_4}} \\ &= \frac{1}{2} (s_1 s_2 + 1) \frac{1}{2} (s_2 s_3 + 1) \frac{1}{2} (s_3 s_4 + 1) \\ &= \frac{1}{8} (s_1 s_2^2 s_3^2 s_4 + s_1 s_2^2 s_3 + s_1 s_2 s_3 s_4 + s_1 s_2 \\ &\quad + s_2 s_3^2 s_4 + s_2 s_3 + s_3 s_4 + 1) \\ &= \frac{1}{8} [s_4 (s_1 + s_2 + s_3 + s_1 s_2 s_3) \\ &\quad + s_1 s_2 + s_1 s_3 + s_2 s_3 + 1] \\ &\rightarrow \frac{1}{8} [s_4 (s_1 + s_2 + s_3 + s_1 s_2 s_3) + s_1 s_2 + s_1 s_3 + s_2 s_3] \\ &\rightarrow \frac{1}{8} [s_4 (s_1 + s_2 + s_3 + s_1 s_2 s_3) + s_4 s_2 + s_4 s_3 + s_4 s_3] \\ &\rightarrow \frac{1}{8} s_4 (s_1 + 2s_2 + 3s_3 + s_1 s_2 s_3), \end{aligned} \quad (18)$$

where we have used a right arrow, rather than the equal sign, to indicate functional, but not formal, equality. Similarly, for $k = 5$, one gets

$$S^{(5)} = \frac{1}{16} s_5 (s_1 + 2s_2 + 3s_3 + 4s_4 + s_1 s_2 s_3 + s_1 s_2 s_4 + s_1 s_3 s_4 + 2s_2 s_3 s_4), \quad (19)$$

and for $k = 6$ it is

$$S^{(6)} = \frac{1}{32} s_6 (s_1 + 2s_2 + 3s_3 + 4s_4 + 5s_5 + s_1 s_2 s_3 + s_1 s_2 s_4 + s_1 s_2 s_5 + s_1 s_3 s_4 + s_1 s_3 s_5 + s_1 s_4 s_5 + 2s_2 s_3 s_4 + 2s_2 s_3 s_5 + 2s_2 s_4 s_5 + 3s_3 s_4 s_5 + s_1 s_2 s_3 s_4 s_5). \quad (20)$$

It becomes then clear that the vector expression for

$$\sigma_{\xi_1, \xi_2, \dots, \xi_{k-1}} = \sum_{\substack{r=1 \\ r \text{ odd}}}^{k-1} \sum_{\substack{\text{ordered } r\text{-choices} \\ \text{from } \{\zeta_1, \zeta_2, \dots, \zeta_{k-1}\}}} \alpha_1 \zeta_1 \zeta_2 \cdots \zeta_r \Big|_{\zeta_1 = s_{\xi_1}, \zeta_2 = s_{\xi_2}, \dots, \zeta_{k-1} = s_{\xi_{k-1}}}, \quad (23)$$

where α_1 is the ordinal index of ζ_1 , so that $\alpha_1 = 1$ if $\zeta_1 = \zeta_1$, $\alpha_1 = 2$ if $\zeta_1 = \zeta_2$, and so on.

Note that this demonstration not only offers a straightforward way to employ spectral methods in search of the best partition of a higher-order network into two communities, but it also shows that in classification tasks, the assignment corresponding to the first higher-order singular vector of a data tensor is indeed the best one, and not just an approximation of it, in turn providing an explanation of the success of methods based on higher-order SVD in machine learning.

E. Repeated bisections

When searching for the best partition of a network, it is clear that, in general, it may not consist of just two communities. A natural idea is then to apply the same method to the communities resulting from an initial partitioning, checking whether hypermodularity increases when splitting those even further. However, care must be taken when doing so. The reason is that a key step in the derivation of Eq. 21 and Eq. 23 relies on the vanishing of the sum of all elements of \mathbf{B} . However, bisecting an already existing community, this condition is no longer true, as one works with the subtensor corre-

sponding to the nodes in the community, rather than with the data tensor of the entire network.

$$Q = \frac{1}{2^{k-1} k! m} \mathbf{s}^T \mathbf{E} \boldsymbol{\sigma}^{(k)}, \quad (21)$$

where $\boldsymbol{\sigma}^{(k)}$ is a vector with N^{k-1} components that can be written as

$$\boldsymbol{\sigma}^{(k)} = (\sigma_{1,1,\dots,1}, \sigma_{2,1,\dots,1}, \sigma_{3,1,\dots,1}, \dots, \sigma_{N,1,\dots,1}, \sigma_{1,2,\dots,1}, \sigma_{2,2,\dots,1}, \sigma_{3,2,\dots,1}, \dots, \sigma_{N,N,\dots,N})^T. \quad (22)$$

Here, the elements of $\boldsymbol{\sigma}^{(k)}$ are characterized by $k - 1$ indices whose sequence is in inverse lexicographic order, and their actual values are given by

sponding to the nodes in the community, rather than with the data tensor of the entire network.

To find the correct way to deal with this situation, consider the change in hypermodularity that would result from a further split of a community C . This can be expressed as the sum of a positive term coming from the new split and a negative one, which is the contribution of the nodes in the community to the current value of the hypermodularity. From Eq. 3, it is clear that the former term consists of all and only the elements of the subtensor of C that correspond to nodes assigned to the same community. Similarly, the latter term is the sum of all the element of the same subtensor. Thus, it is

$$\Delta Q = \frac{1}{k! m} \left(\sum_{k\text{-sets in } C} B_{v_1, \dots, v_k} \delta_{C_{v_1}, C_{v_2}} \cdots \delta_{C_{v_{k-1}}, C_{v_k}} - \sum_{k\text{-sets in } C} B_{v_1, \dots, v_k} \right). \quad (24)$$

Now, write the product of deltas in terms of the spin-like variables, as before. However, note that, for the reasons discussed above, the constant term can no longer be neglected. This results in

$$\Delta Q = \frac{1}{k! m} \left[\frac{1}{2^{k-1}} \sum_{s_{v_1}} \cdots \sum_{s_{v_k}} B_{v_1, \dots, v_k} (s_{v_k} f(s_{v_1}, \dots, s_{v_{k-1}}) + 1) - \sum_{s_1} \cdots \sum_{s_{v_k}} B_{v_1, \dots, v_k} \right], \quad (25)$$

where we have explicitly expanded the sums and f is a

polynomial in the first $k - 1$ spin-like variables, as in

Eq. (16) and in Eqs. (18-20).

Then, expanding the product, we obtain

$$\begin{aligned}
\Delta Q &= \frac{1}{k!m} \left(\frac{1}{2^{k-1}} \sum_{s_{v_1}} \cdots \sum_{s_{v_k}} B_{v_1, \dots, v_k} s_{v_k} f(s_{v_1}, \dots, s_{v_{k-1}}) + \frac{1}{2^{k-1}} \sum_{s_{v_1}} \cdots \sum_{s_{v_k}} B_{v_1, \dots, v_k} - \sum_{s_{v_1}} \cdots \sum_{s_{v_k}} B_{v_1, \dots, v_k} \right) \\
&= \frac{1}{k!m} \left(\frac{1}{2^{k-1}} \sum_{s_{v_1}} \cdots \sum_{s_{v_k}} B_{v_1, \dots, v_k} s_{v_k} f(s_{v_1}, \dots, s_{v_{k-1}}) - \frac{2^{k-1} - 1}{2^{k-1}} \sum_{s_{v_1}} \cdots \sum_{s_{v_k}} B_{v_1, \dots, v_k} \right) \\
&= \frac{1}{2^{k-1} k!m} \left[\sum_{s_{v_1}} \cdots \sum_{s_{v_k}} B_{v_1, \dots, v_k} s_{v_k} f(s_{v_1}, \dots, s_{v_{k-1}}) - (2^{k-1} - 1) \sum_{s_{v_1}} \cdots \sum_{s_{v_k}} B_{v_1, \dots, v_k} \right] \\
&= \frac{1}{2^{k-1} k!m} \left[\sum_{s_{v_1}} \cdots \sum_{s_{v_k}} B_{v_1, \dots, v_k} s_{v_k} f(s_{v_1}, \dots, s_{v_{k-1}}) \right. \\
&\quad \left. - (2^{k-1} - 1) \sum_{s_{v_1}} \cdots \sum_{s_{v_k}} \delta_{v_1, v_2} \cdots \delta_{v_{k-1}, v_k} \sum_{s_{w_1}} \cdots \sum_{s_{w_{k-1}}} B_{w_1, \dots, w_{k-1}, v_k} \right] \\
&= \frac{1}{2^{k-1} k!m} \left[\sum_{s_{v_1}} \cdots \sum_{s_{v_k}} B_{v_1, \dots, v_k} s_{v_k} f(s_{v_1}, \dots, s_{v_{k-1}}) \right. \\
&\quad \left. - (2^{k-1} - 1) \sum_{s_{v_1}} \cdots \sum_{s_{v_k}} \delta_{v_1, v_2} \cdots \delta_{v_{k-1}, v_k} \sum_{s_{w_1}} \cdots \sum_{s_{w_{k-1}}} B_{w_1, \dots, w_{k-1}, v_k} \frac{s_{v_k} f(s_{v_1}, \dots, s_{v_{k-1}})}{2^{k-1} - 1} \right], \tag{26}
\end{aligned}$$

where, in the last line, we have used the fact that

$$s_{v_k} f(s_{v_1}, \dots, s_{v_{k-1}}) = 2^{k-1} - 1 \text{ when } v_1 = v_2 = \cdots = v_k.$$

But then, it is

$$\Delta Q = \frac{1}{2^{k-1} k!m} \sum_{s_{v_1}} \cdots \sum_{s_{v_k}} s_{v_k} \left(B_{v_1, \dots, v_k} - \delta_{v_1, v_2} \cdots \delta_{v_{k-1}, v_k} \sum_{s_{w_1}} \cdots \sum_{s_{w_{k-1}}} B_{w_1, \dots, w_{k-1}, v_k} \right) f(s_{v_1}, \dots, s_{v_{k-1}}), \tag{27}$$

which means that we can express the change in hypermodularity as the vector equation

$$\Delta Q = \frac{1}{2^{k-1} k!m} \mathbf{s}^T \mathbf{E}' \boldsymbol{\sigma}^{(k)}, \tag{28}$$

where \mathbf{E}' is the flattening of a modified community sub-tensor \mathbf{B}' , obtained by adding a correction to the elements on the main hyperdiagonal:

$$B'_{v_1, \dots, v_k} = \begin{cases} B_{v_1, \dots, v_k} - \sum_{s_{w_1}} \cdots \sum_{s_{w_{k-1}}} B_{w_1, \dots, w_{k-1}, v_k} & \text{if } v_1 = v_2 = \cdots = v_k \\ B_{v_1, \dots, v_k} & \text{otherwise.} \end{cases} \tag{29}$$

Note that the correction terms vanish if one considers the whole network, as expected. Thus, one can always directly use Eq. (28), since it reduces to Eq. (21) when the network has not yet been partitioned.

Using the formalism just described, we build an algorithm that searches for the best partition of a k -uniform higher-order network into communities by carrying out repeated bisections. Following the approach of Refs. [26] and [41], we also include refinement steps, which we briefly describe below.

F. Refinement steps

After operating a bisection, we carry out a first refinement by computing how the hypermodularity would change if one were to switch the placement of each node from the community to which it was assigned to the other one. All the nodes are considered, and then, in a greedy fashion, the best move is accepted. The remaining nodes are then considered again, and the best move is accepted each time, until all the nodes have been evaluated. The best middle point throughout the proce-

ture is then found. If it corresponds to an increase in hypermodularity, the moves up to that point are permanently accepted; otherwise, the state of the network is reverted to the one at the start of the procedure. The refinement is then repeated until no further improvement is obtained.

To compute the change in hypermodularity that each move would yield, first note that changing the assignment of a single node i results in a single element of the vector \mathbf{s} to switch sign. Similarly, the vector $\boldsymbol{\sigma}^{(k)}$ only changes in the elements that correspond to combinations of $k-1$ nodes involving node i . Thus, we can write $\boldsymbol{\sigma}^{(k)} \rightarrow \boldsymbol{\sigma}'^{(k)} = \boldsymbol{\sigma}^{(k)} + \Delta\boldsymbol{\sigma}^{(k)}$ and $\mathbf{s} \rightarrow \mathbf{s}' = \mathbf{s} + \Delta\mathbf{s}$, where all the elements of $\Delta\mathbf{s}$ are 0, except for the i -th one, which is equal to $-2s_i$. Then, write the hypermodularity of the partition after the change as

$$\begin{aligned} Q' &= \frac{1}{2^{k-1}k!m} (\mathbf{s} + \Delta\mathbf{s})^T \mathbf{E}' (\boldsymbol{\sigma}^{(k)} + \Delta\boldsymbol{\sigma}^{(k)}) \\ &= \frac{1}{2^{k-1}k!m} \left(\mathbf{s}^T \mathbf{E}' \boldsymbol{\sigma}^{(k)} + \mathbf{s}^T \mathbf{E}' \Delta\boldsymbol{\sigma}^{(k)} \right. \\ &\quad \left. + \Delta\mathbf{s}^T \mathbf{E}' \boldsymbol{\sigma}^{(k)} + \Delta\mathbf{s}^T \mathbf{E}' \Delta\boldsymbol{\sigma}^{(k)} \right). \end{aligned} \quad (30)$$

From this equation, it follows that

$$\begin{aligned} \Delta Q &= \frac{1}{2^{k-1}k!m} \left(\mathbf{s}^T \mathbf{E}' \Delta\boldsymbol{\sigma}^{(k)} + \Delta\mathbf{s}^T \mathbf{E}' \boldsymbol{\sigma}^{(k)} \right. \\ &\quad \left. + \Delta\mathbf{s}^T \mathbf{E}' \Delta\boldsymbol{\sigma}^{(k)} \right) \\ &= \frac{1}{2^{k-1}k!m} \left(\mathbf{s}'^T \mathbf{E}' \Delta\boldsymbol{\sigma}^{(k)} + \Delta\mathbf{s}^T \mathbf{E}' \boldsymbol{\sigma}^{(k)} \right). \end{aligned} \quad (31)$$

This form is particularly convenient, because the vector $\boldsymbol{\sigma}^{(k)}$ is already known from the previous step. Thus, the second term can be readily computed as the product of the i -th row of \mathbf{E}' and $\boldsymbol{\sigma}^{(k)}$, multiplied by $-2s_i$, and the first term can be calculated similarly, by accounting for all and only the combinations of factors that include node i .

After all existing communities have been evaluated for further splits, and the local node-level refinement has been considered, we perform a global node-level optimization. The structure of this step is again that of an iterated greedy algorithm that evaluates the change in hypermodularity resulting from moving each node from the community to which it is currently assigned to any other possible community. As before, the best move is accepted, and the evaluation is repeated for the remaining nodes, until all nodes have been moved. Then, the middle point in the sequence of moves corresponding to the largest change in hypermodularity is found, and the all the moves up to that point are permanently accepted if such change is positive. The step is repeated until it produces an improvement in hypermodularity.

The change in hypermodularity caused by moving node i to community α consists of two contributions. The first is a negative one, which is due to all and only the combinations of k nodes in the original community of i

such that at least one of them is node i itself. The second is a positive change that is due to all and only the combinations of k -nodes in community α , with the temporary inclusion of node i within it, such that at least one of them is node i itself. Both are sums of the elements of \mathbf{B} corresponding to the combinations of nodes taken, divided by $k!m$, and with the sign of the negative contribution changed.

Finally, if the current partition consists of more than 1 community, a community-level optimization is carried out. As for the previous two steps, also this is an iterated greedy algorithm, repeated so long as the value of hypermodularity increases. The moves considered are the mergings of pairs of communities, akin to the main procedure of the Louvain algorithm [20]. Merging community α and community β causes a change in hypermodularity that is due to all and only the combinations of k nodes such that at least one is in community α and one is in community β . As in the previous step, each combination contributes an amount equal to the corresponding element of \mathbf{B} divided by $k!m$. This means that the potential changes in hypermodularity can be represented as a matrix whose dimension is the current number of communities. When a move is accepted, it is convenient to take all the nodes belonging to the community with the higher index and assign them to the other one. This way, for all subsequent moves, the only matrix elements that change are those involving the community with the lower index, and, because of symmetry, only half a row and half a column need to be updated.

G. Numerical validation

To demonstrate the applicability of the method, we implemented the algorithm described above, and analyzed both synthetic and real-world higher-order networks. We started with the study of ensembles of Erdős-Rényi-like random k -uniform hypergraphs, to determine the behaviour of hypermodularity on networks without a well-defined community structure. In these networks, every possible hyperedge of size k exists independently with the same probability p . We ran the algorithm on networks of size 10, 20, 50 and 100, with $k = 3$ and $k = 4$. The behaviour of the average maximum hypermodularity as a function of p , shown in Fig. 1, shows that, on connected networks, the best partition never corresponds, on average, to a hypermodularity greater than 0.2. However, as the connection probability decreases, and the networks start fragmenting into separate connected components, the maximum value of the hypermodularity increases even as high as 0.8. At first, this may seem evidence of a problem with the measure, as there appear to exist partitions of completely random networks whose hypermodularity is close to the theoretical maximum of 1. However, such values are actually spurious and they are, in fact, due to the fragmentation of the networks.

To understand how this happens, consider a limit case

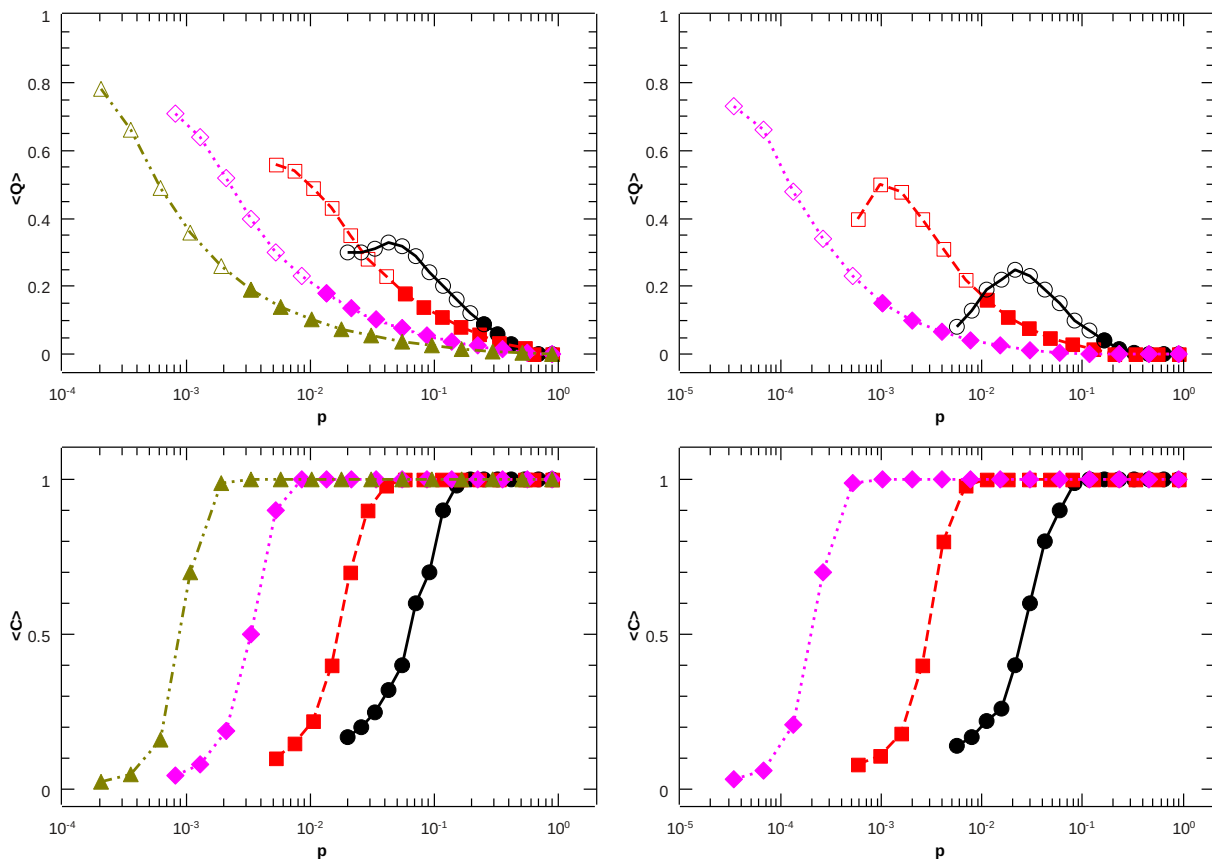


Figure 1. **Maximum hypermodularity in random hypergraphs is never above 0.2.** So long as the networks remain connected, the average maximum hypermodularity $\langle Q \rangle$ of random k -uniform hypergraphs remains below 0.2, as shown here for $k = 3$ (left-hand top panel) and $k = 4$ (right-hand top panel). As the connection probability p decreases, the networks start to fragment, and the value of the maximum hypermodularity spuriously increases (empty symbols). The bottom panels show the average fraction of nodes in the components of the networks $\langle C \rangle$. For all panels, black circles and solid lines correspond to $N = 10$, red squares and dashed lines to $N = 20$, purple diamonds and dotted lines to $N = 50$ and green triangles and dotted-and-dashed lines to $N = 100$.

of a hypergraph formed by m isolated hyperedges. Its maximum hypermodularity, which is found by assigning all the nodes of each edge to a separate community, is $1 - \frac{(k-1)!}{(km)^{k-1}}$, which, for large m , is approximately 1. However, the hypermodularity of the individual components, which consist each of a single edge, is identically 0. This shows that one must be very careful in using hypermodularity on networks that are not connected, and that in such cases the right approach is to treat each component as an independent network. Thus, our results also indicate that concerns of overfitting, as have been occasionally voiced also for traditional modularity, are mostly unfounded, and one can take the value of 0.2 as a sort of physiological expected maximum hypermodularity of a random network, due to the non-vanishing probability that, even in a random structure, some sets of nodes may be more densely linked internally than they are between each other.

We then tested the method on real-world data sets, using contact information from a primary school [42, 43]

and from a high school [43, 44]. In the former case, the pupils are classified according to their grade, with two separate classes running for each year from 1 to 5. The teachers, one per class, were also involved in the study. The high-school students, instead, are classified according to the topic of the classes they were following. Specifically, the data set contains three classes of biology, three of mathematics and physics, two of chemistry and one of psychology. In both cases, we detected the community structure for edges of sizes 2 to 5, since no edges of larger size were recorded.

The primary school results, shown in Fig. 2, are quite revealing. When we use $k = 2$, which corresponds to a traditional network, the algorithm divides the students into 5 communities, each corresponding to a different grade, with the exception that all the pupils of one of the classes of year 4 are assigned to the same community as the pupils of year 5. This partition, with a modularity of 0.3066, is consistent with younger children tending to separate by age in their individual interactions, and with such boundaries becoming less rigid as they grow up.

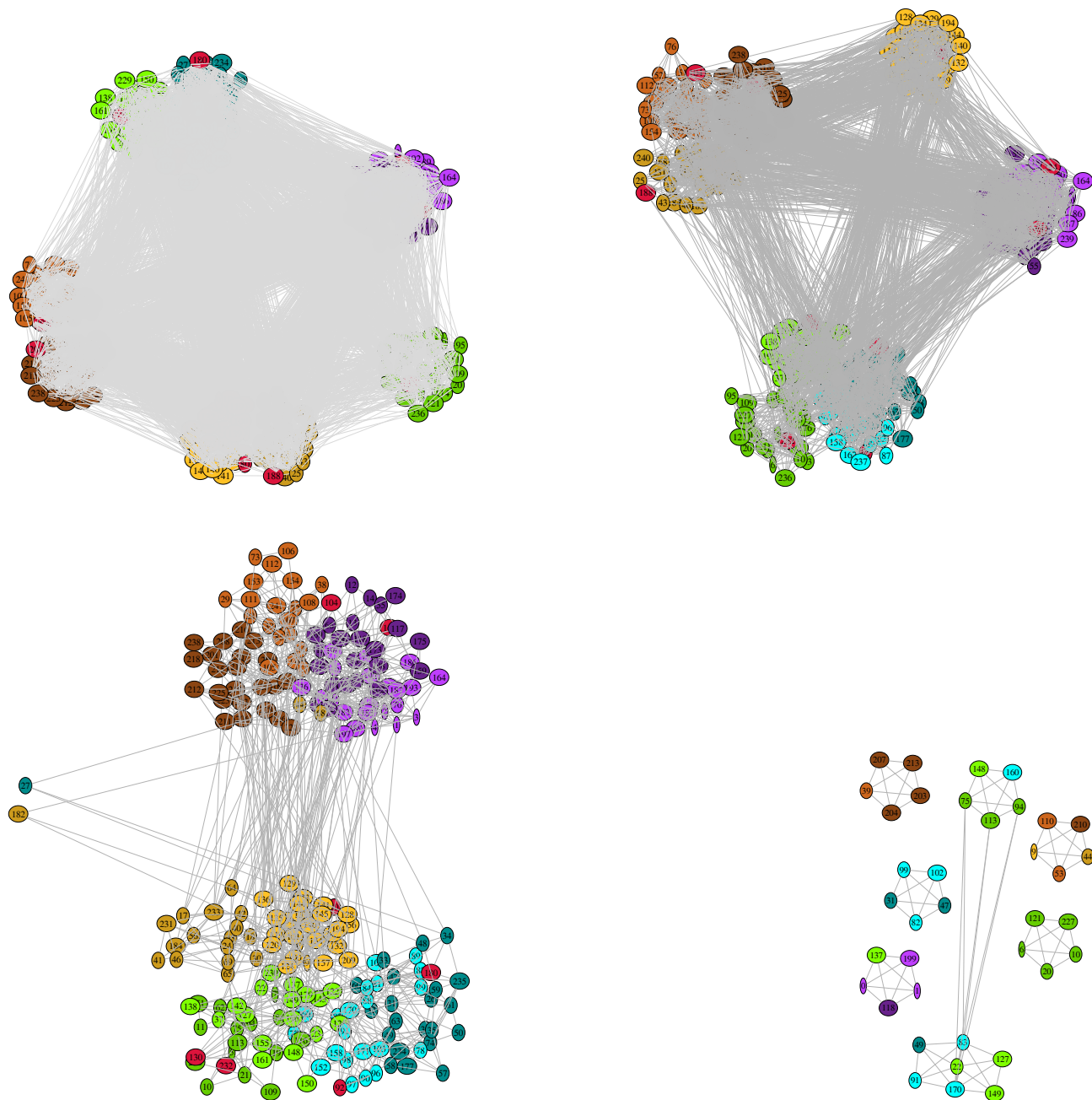


Figure 2. **Higher-order communities of primary-school pupils reveal underlying social dynamics.** The communities of 2-person and 3-person interactions (top-left and top-right panels, respectively) show that tight-group interactions between primary-school pupils mostly occur within age groups. Communities of looser groups of 4 people (bottom-left) blur this line, with younger siblings being accepted within groups of older children. Finally, interactions of 5 pupils at a time (bottom-right) are rare, and possibly stronger, thereby restoring the age separation seen for $k = 2$ and $k = 3$. In all panels, yellow nodes correspond to pupils in year 1, brown nodes to pupils in year 2, violet nodes to pupils in year 3, green nodes to pupils in year 4, blue nodes to pupils in year 5 and red nodes to teachers. Each year consists of two separate classes, signified by the shade of the colour. Note that in preparing the figure, hyperedges ($k > 2$) have been projected onto cliques for ease of visualization.

The communities of 3-people interactions ($k = 3$) reveal a similar situation. Year-3 students keep to themselves, whereas one entire class of year-1 pupils joins the two of year-2 students to form a community. The pupils of the last two years are together in the same community. This division, with a hypermodularity of 0.71, is again consistent with the dynamics just described. Year-3 students consider the two lower grades too young to form social interactions with, and they are themselves considered too young by the two higher grades. The data for $k = 4$ show an intriguing division, with a hypermodularity of 0.7632. Years 2 and 3 are joined in a single community, and years 1, 4 and 5 form another one, with two individual isolated students. A possible explanation for the former is that in looser groups of four people it is easier to include one or two members of different age without introducing too much disparity of maturity than it is in tighter groups of 2 or 3 people. The latter community is perhaps more striking. The age difference between the individuals in year 1 and those in year 4 and year 5 is of 3 to 4 years, and this community seems to result from the presence of siblings, who join the age-based social group of their brothers and sisters. Indeed, the average age gap between siblings in the period where the data were collected was, in fact, 3.5 years [45]. Finally, for $k = 5$ the network is almost completely fragmented, and the only nodes left with some edges separate into communities that are either uniform, or with at most one grade of difference between the members. Note that the network of 5-people interactions consists of 6 components, 5 of which contain a single hyperedge, and thus have a vanishing hypermodularity. The division of the only non-trivial component has a hypermodularity of 0.662.

The analysis of the high-school data set, shown in Fig. 3, also provides insights into the social dynamics of the groups of students. When one considers only dyadic interactions, the network separates into communities that are completely identified not only by the topic studied, but also by the specific class in which the students are enrolled. This partition has a modularity of 0.5915, and the only exception is that the mathematics and physics students form a single community, rather than splitting into their three classes. This evidently disproves the stereotype that sees mathematics and physics students as socially inept. In fact, in this study, they are the only group of people that socialize across classes, albeit in the same topic. When we take $k = 3$, the network is very highly modular, with 3 large communities plus an individual node and a hypermodularity of 0.8313. Here, the communities are entirely topic-based, but the students of psychology are joined with those of mathematics and physics. A possible explanation for this is that both physicists and psychologists study complex systems, even though using different means of representation. Thus, they have a larger affinity than one may imagine at a first thought. At the next larger size of edges, $k = 4$, the meta-group of mathematics-physics-psychology students joins that of chemistry ones, with the notable exception

of 9 mathematics-and-physics students who are now assigned to the community of biology. Also, the network starts fragmenting, with an isolated clique of 5 biology students. This partition of the large component has a hypermodularity of 0.8527, and it is mostly caused by a few students who act as bridges between disciplines, and whose importance increases as the network has substantially fewer edges. For example, psychology student 325 is well connected with other psychology students and with mathematics-physics ones, chemistry student 284 is highly connected with a clique of psychology students and with numerous other chemistry ones, and mathematics-physics students 125 and 176 have several links to other students in the same class as well as to biology ones. Finally, when $k = 5$ very few nodes remain with some edges. Five of them are a clique of chemistry students, and the other three components consist entirely of students of the same topic (two components for biology and one for chemistry). This suggests that these components are study groups, and the larger communities identified within them are their core members. It should be noted, nonetheless, that only the larger biology component is reasonably modular, with its partition corresponding to a hypermodularity of 0.3319, whereas both other components have a hypermodularity of 0.1723, which is below what one would expect from a random hypergraph, as discussed above.

III. CONCLUSIONS

In this article, we have considered the task of detecting communities in networks with interactions beyond pairwise ones. Our way to attack this problem consists in defining a hypermodularity function for hypergraphs using a formalism that is conducive to the use of spectral methods to find the bisection of the network that maximizes it. Specifically, we have shown that this can be achieved by the use of higher-order singular value decomposition, if one rewrites the condition that the elements of a given set of nodes all belong to the same community as a separable expression of spin-like variables. To do so, we demonstrated a closed combinatorial expression that allows one to ultimately turn the hypermodularity equation into a vector form.

After implementing an algorithm based on these ideas, we applied it to random hypergraphs, finding a physiological value of maximum hypermodularity that one can expect to find in networks without an imposed community structure. This is due to the non-zero probability that, even placing all edges at random, one can end up with modules of nodes whose internal edges are denser than their external ones. Notably, the hypermodularity of random hypergraphs never exceeded 0.2, suggesting that this value can be considered as a rough threshold to determine the presence of strong communities.

When applied to real-world data, our algorithm was able to detect communities at different levels of collective

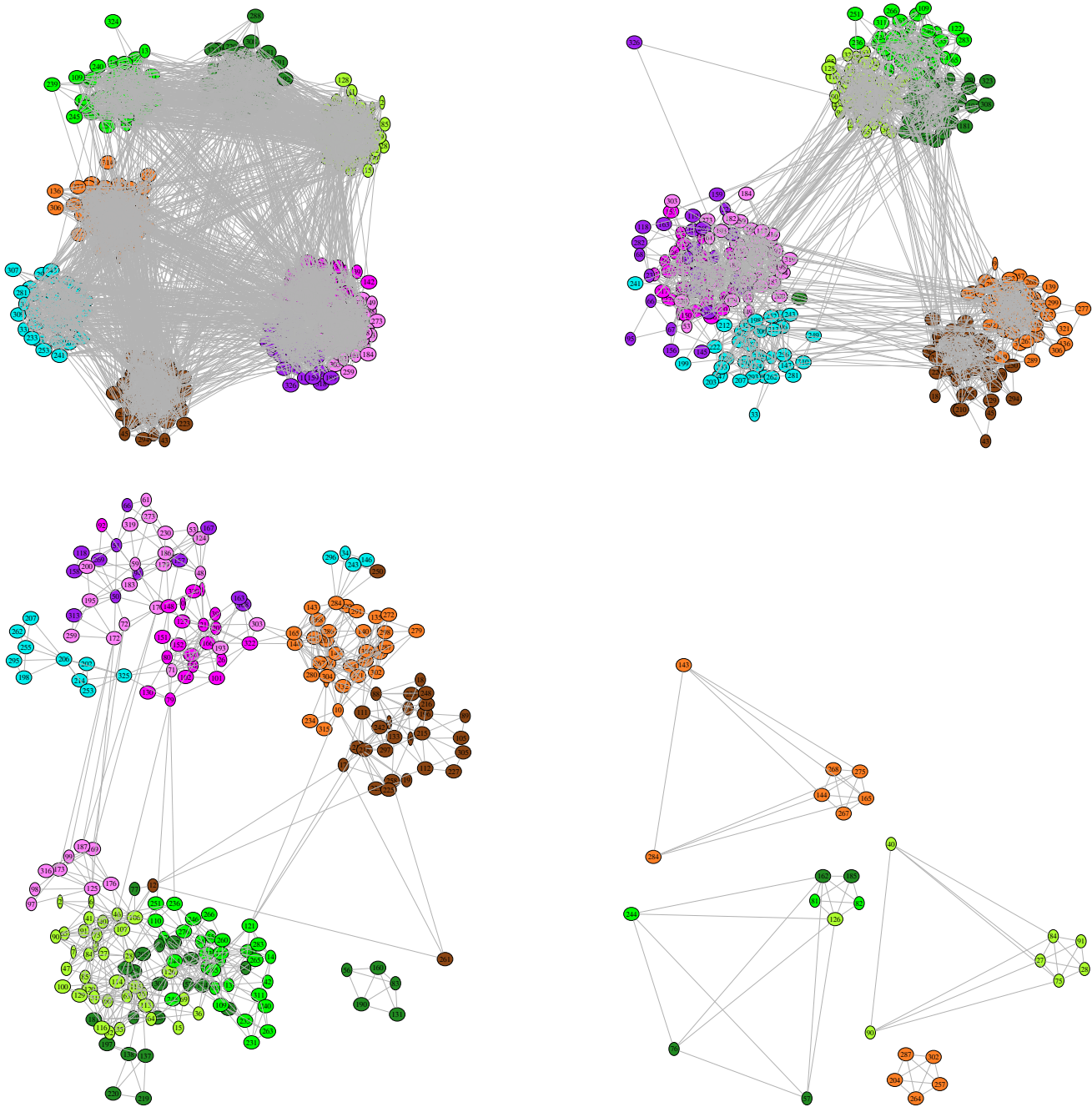


Figure 3. **Higher-order communities of high-school students provide insights into closeness of interests.** The communities of dyadic interactions between high-school students (top-left) show a strong division between topics (colours) and classes (shades), with the exception of mathematics and physics students (violet), who interact across classes, challenging the stereotypical opinion of more mathematically minded people being unable to form meaningful social contacts. The communities of groups of 3 people (top-right) reveal the proximity of thought between psychology and mathematics-physics students, who are now joined in a single community. The 4-people interactions (bottom-left) extend this insight, revealing how biology students (green) are substantially isolated, whereas almost all the other students belong to the same community, with the exception of a small separate clique. Finally, at $k = 5$ the network consists of only 4 small study groups. In all panels, green nodes correspond to biology students, violet nodes to mathematics and physics students, brown nodes to chemistry students and blue nodes to psychology students. All topics except psychology include more than one class, signified by the shade of the colour. Note that in preparing the figure, hyperedges ($k > 2$) have been projected onto cliques for ease of visualization.

interaction. The communities thus identified can all be explained by assuming reasonable mechanisms for their formation. In fact, it can be argued that the communities found on social contact networks represent similarity of thought processes and reflect the biases of the individuals. Thus, we believe that our formulation of hypermodularity and our algorithm constitute powerful tools for the analysis of networks with higher-order interactions, and are highly valuable methods for extracting hidden information from data sets of diverse nature.

ACKNOWLEDGMENTS

The author acknowledges fruitful discussions with Ekaterina Vasilyeva and Stefano Boccaletti. This work was supported by the Bulgarian Ministry of Education and Science under project number BG-RRP-2.004-0006-C02.

-
- [1] R. Albert and A.-L. Barabási, Statistical mechanics of complex networks, *Rev. Mod. Phys.* **74**, 47 (2002).
- [2] M. E. J. Newman, Structure and function of complex networks, *SIAM Rev.* **45**, 167 (2003).
- [3] S. Boccaletti, V. Latora, Y. Moreno, M. Chavez and D.-U. Hwang, Complex networks: structure and dynamics, *Phys. Rep.* **424**, 175 (2006).
- [4] S. Boccaletti, G. Bianconi, R. Criado, C. I. del Genio, J. Gómez-Gardeñes, M. Romance, I. Sendiña-Nadal, Z. Wang and M. Zanin, The structure and dynamics of multilayer networks, *Phys. Rep.* **544**, 1 (2014).
- [5] S. L. Pimm, Structure of food webs, *Theor. Popul. Biol.* **16**, 144 (1979).
- [6] G. P. Garnett, J. P. Hughes, R. M. Anderson, B. P. Stoner, S. O. Aral, W. L. Whittington, H. H. Handfield and K. K. Holmes, Sexual mixing patterns of patients attending sexually transmitted diseases clinics, *Sex. Transm. Dis.* **23**, 248 (1996).
- [7] G. W. Flake, S. Lawrence, C. L. Giles and F. M. Coetzee, Self-organization and identification of web communities, *Computer* **32**, 66 (2002).
- [8] K. A. Eriksen, I. Simonsen, S. Maslov and K. Sneppen, Modularity and extreme edges of the internet, *Phys. Rev. Lett.* **90**, 148701 (2003).
- [9] A. E. Krause, K. A. Frank, D. M. Mason, R. E. Ulanowicz and W. W. Taylor, Compartments revealed in food-web structure, *Nature* **426**, 282 (2003).
- [10] D. Lusseau and M. E. J. Newman, Identifying the role that animals play in their social networks, *Proc. R. Soc. Lond. B Biol.* **271**, S477 (2004).
- [11] R. Guimerà and L. A. N. Amaral, Functional cartography of complex metabolic networks, *Nature* **433**, 895 (2005).
- [12] G. Palla, I. Derényi, I. Farkas and T. Vicsek, Uncovering the overlapping community structure of complex networks in nature and society, *Nature* **435**, 814 (2005).
- [13] M. Huss and P. Holme, Currency and commodity metabolites: their identification and relation to the modularity of metabolic networks, *IET Syst. Biol.* **1**, 280 (2007).
- [14] S. Fortunato, Community structure in graphs, *Phys. Rep.* **486**, 75 (2010).
- [15] H. Cherifi, G. Palla, B. K. Szymanski and X. Lu, On community structure in complex networks: challenges and opportunities, *Appl. Netw. Sci.* **4**, 117 (2019).
- [16] M. E. J. Newman, Modularity and community structure in networks, *Proc. Natl. Acad. Sci. USA* **103**, 8577 (2006).
- [17] U. Brandes, D. Delling, M. Gaertler, R. Görke, M. Hofer, Z. Nikoloski and D. Wagner, *IEEE T. Knowl. Data En.* **20**, 172 (2008).
- [18] M. Chen, K. Kuzmin and B. K. Szymanski, Community detection via maximization of modularity and its variants, *IEEE Trans. Comput. Soc. Syst.* **1**, 46 (2004).
- [19] J. Duch and A. Arenas, Community detection in complex networks using extremal optimization, *Phys. Rev. E* **72**, 027104 (2005).
- [20] V. D. Blondel, J. L. Guillaume, R. Lambiotte and E. Lefebvre, Fast unfolding of communities in large networks, *J. Stat. Mech. Theory E.*, P10008 (2008).
- [21] A. Noack and R. Rotta, Multi-level algorithms for modularity clustering, *Lect. Notes Comput. Sci.* **5526**, 257 (2009).
- [22] Y. Sun, B. Danila, K. Josić and K. E. Bassler, Improved community structure detection using a modified fine-tuning strategy, *EPL* **86**, 2009.
- [23] B. H. Good, Y.-A. de Montjoye and A. Clauset, Performance of modularity maximization in practical contexts, *Phys. Rev. E* **81**, 046106 (2010).
- [24] E. Le Martelot and C. Hankin, Multi-scale community detection using stability as optimisation criterion in a greedy algorithm, *Proc. Int. Conf. Knowledge Discovery and Information Retrieval (KDIR 2011)*, 216 (2011).
- [25] S. Sobolevsky, R. Campari, A. Belyi and C. Ratti, General optimization technique for high-quality community detection in complex networks, *Phys. Rev. E* **90**, 012811 (2014).
- [26] S. Treviño III, A. Nyberg, C. I. del Genio and K. E. Bassler, Fast and accurate determination of modularity and its effect size, *J. Stat. Mech. Theory E.*, P02003 (2015).
- [27] X. Lu, B. Cross and B. Szymanski, Asymptotic resolution bounds of generalized modularity and multi-scale community detection, *Inform. Sciences* **525**, 54 (2020).
- [28] F. Battiston, G. Cencetti, I. Iacopini, V. Latora, M. Lucas, A. Patania, J.-G. Young and G. Petri, Networks beyond pairwise interactions: structure and dynamics, *Phys. Rep.* **874**, 1 (2020).
- [29] S. Boccaletti, P. De Lellis, C. I. del Genio, K. Alfaro-Bittner, R. Criado, S. Jalan and M. Romance, The structure and dynamics of networks with higher order interactions, *Phys. Rep.* **1018**, 1 (2023).
- [30] C. Berge, *Graphs and hypergraphs* (Elsevier, 1973).
- [31] M. C. Angelini, F. Caltagirone, F. Krzakala and L. Zdeborová, Spectral detection on sparse hypergraphs, *Proc. 2015 53rd Ann. Allerton Conf. Commun. Control Comp.*, 66 (2015).
- [32] T. Kumar, S. Vaidyanathan, H. Ananthapadmanabhan, S. Parthasarathy and B. Ravindran, Hypergraph cluster-

- ing by iteratively reweighted modularity maximization, *Appl. Net. Sci.* **5**, 52 (2020).
- [33] A. Eriksson, T. Carletti, R. Lambiotte, A. Rojas and M. Rosvall, Flow-based community detection in hypergraphs, in F. Battiston and G. Petri (eds.), “Higher-order systems” (Springer, 2022).
- [34] G. Contreras-Aso, R. Criado, G. Vera de Salas and J. Yang, Detecting communities in higher-order networks by using their derivative graphs, *Chaos Soliton. Fract.* **177**, 114200 (2023).
- [35] B. Kamiński, V. Poulin, P. Prałat, P. Szufel and F. Théberge, Clustering via hypergraph modularity, *PLoS One* **14**, e0224307 (2019).
- [36] A. Rajwade, A. Rangarajan and A. Banerjee, Image denoising using the higher order singular value decomposition, *IEEE T. Pattern Anal.* **35**, 849 (2013).
- [37] P. Sankaranarayanan, T. E. Schomay, K. A. Aiello and O. Alter, Tensor GSVD of patient- and platform-matched tumor and normal DNA copy-number profiles uncovers chromosome arm-wide patterns of tumor-exclusive platform-consistent alterations encoding for cell transformation and predicting ovarian cancer survival, *PLoS One* **10**, e0121396 (2015).
- [38] Y. H. Taguchi, Identification of candidate drugs using tensor-decomposition-based unsupervised feature extraction in integrated analysis of gene expression between diseases and DrugMatrix datasets, *Sci. Rep.* **7**, 13733 (2017).
- [39] Y. H. Taguchi, Tensor decomposition-based unsupervised feature extraction applied to matrix products for multi-view data processing, *PLoS One* **13**, e0200451 (2017).
- [40] B. Vilas Boas, W. Zirwas and M. Haardt, Deep-LaRGE: higher-order SVD and deep learning for model order selection in MIMO OFDM systems, *Proceedings of the 26th International ITG Workshop on Smart Antennas and 13th Conference on Systems, Communications, and Coding, Braunschweig*, 1 (2023).
- [41] F. Botta and C. I. del Genio, Finding network communities using modularity density, *J. Stat. Mech. Theory E.*, 123402 (2016).
- [42] J. Stehlé, N. Voirin, A. Barrat, C. Cattuto, L. Isella, J.-F. Pinton, M. Quaggiotto, W. Van den Broeck, C. Régis, B. Lina and P. Vanhems, High-Resolution Measurements of Face-to-Face Contact Patterns in a Primary School, *PLoS One* **6**, e23176 (2011).
- [43] P. S. Chodrow, N. Veldt and A. R. Benson, Generative hypergraph clustering: From blockmodels to modularity, *Sci. Adv.* **7**, eabh1303 (2021).
- [44] R. Mastrandrea, J. Fournet and A. Barrat, Contact Patterns in a High School: A Comparison between Data Collected Using Wearable Sensors, Contact Diaries and Friendship Surveys, *PLoS One* **10**, e0136497 (2015).
- [45] C. R. Schwartz, C. Doren and A. Li, Trends in Years Spent as Mothers of Young Children: The Role of Completed Fertility, Birth Spacing, and Multiple Partner Fertility, in R. Schoen (ed.), “Analyzing Contemporary Fertility” (Springer, 2020).